



THE UNIVERSITY *of* EDINBURGH

Edinburgh Research Explorer

The kinetic characteristics of human and trypanosomatid phosphofructokinases for the reverse reaction

Citation for published version:

Fernandes, PM, Kinkead, JR, McNae, IW, Michels, PA & Walkinshaw, MD 2019, 'The kinetic characteristics of human and trypanosomatid phosphofructokinases for the reverse reaction' *Biochemical Journal*, vol. 476, no. 2, pp. 179-191. DOI: 10.1042/BCJ20180635

Digital Object Identifier (DOI):

[10.1042/BCJ20180635](https://doi.org/10.1042/BCJ20180635)

Link:

[Link to publication record in Edinburgh Research Explorer](#)

Document Version:

Peer reviewed version

Published In:

Biochemical Journal

Publisher Rights Statement:

Use of open access articles is permitted based on the terms of the specific Creative Commons Licence under which the article is published. archiving of non-open access articles is permitted in accordance with the Archiving Policy of Portland Press (<http://www.portlandpresspublishing.com/content/open-access-policy#archiving>).

General rights

Copyright for the publications made accessible via the Edinburgh Research Explorer is retained by the author(s) and / or other copyright owners and it is a condition of accessing these publications that users recognise and abide by the legal requirements associated with these rights.

Take down policy

The University of Edinburgh has made every reasonable effort to ensure that Edinburgh Research Explorer content complies with UK legislation. If you believe that the public display of this file breaches copyright please contact openaccess@ed.ac.uk providing details, and we will remove access to the work immediately and investigate your claim.



1
2
3
4
5
6
7
8
9
10
11
12
13
14
15
16
17
18
19
20
21
22
23
24
25
26
27
28
29
30
31
32
33
34
35
36
37
38
39
40

TITLE

The kinetic characteristics of human and trypanosomatid phosphofructokinases for the reverse reaction

AUTHORS

Peter M. Fernandes *

James Kinkead *

Iain W. McNae

Paul A.M. Michels,

Malcolm D. Walkinshaw

*These authors contributed equally to this work

Affiliation: School of Biological Sciences, University of Edinburgh, Michael Swann Building, Max Born Crescent, Edinburgh, EH9 3BF, United Kingdom

DISCLOSURES

None declared

FUNDING

PMF was funded by the Wellcome Trust (grant number 106359) and JK by a Wellcome Trust Seeding Drug Discovery grant. Further funding for authors was from a MRC Confidence in Concept grant.

AUTHOR CONTRIBUTION

P.M.F., J.K., I.W.M., P.A.M. and MDW were involved in the conception and design of the experiments and interpretation of the data. P.M.F. and J.K. performed the experiments and prepared the first draft of the manuscript. P.M.F., J.K., P.A.M. and M.D.W. wrote the final version of the manuscript.

CORRESPONDING AUTHOR

MD Walkinshaw: M.Walkinshaw@ed.ac.uk

KEYWORDS

Phosphofructokinase

Human

Trypanosoma cruzi

Trypanosoma brucei

Leishmania

Trypanosomatid

Reverse reaction

41

42 **ABSTRACT**

43 Eukaryotic ATP-dependent phosphofructokinases (PFKs) are often considered unidirectional
44 enzymes catalysing the transfer of a phospho moiety from ATP to fructose 6-phosphate (F6P) to
45 produce ADP and fructose 1,6-bisphosphate (F16BP). The reverse reaction is not generally
46 considered to occur under normal conditions and has never been demonstrated for any eukaryotic
47 ATP-dependent PFKs, though it does occur in P_{Pi}-dependent PFKs and has been experimentally
48 shown for bacterial ATP-dependent PFKs. Evidence is provided via two orthogonal assays that all
49 three human PFK isoforms can catalyse the reverse reaction *in vitro*, allowing determination of kinetic
50 properties. Additionally, the reverse reaction was shown possible for PFKs from three clinically
51 important trypanosomatids; these enzymes are contained within glycosomes *in vivo*. This
52 compartmentalisation may facilitate reversal, given the potential for trypanosomatids to have an
53 altered ATP/ADP ratio in glycosomes compared to the cytosol. The kinetic properties of each
54 trypanosomatid PFK were determined, including the response to natural and artificial modulators of
55 enzyme activity. The possible physiological relevance of the reverse reaction in trypanosomatid and
56 human PFKs is discussed.

57 INTRODUCTION

58 Phosphofructokinase (PFK) catalyses the phosphorylation of fructose 6-phosphate (F6P) to fructose
59 1,6-bisphosphate (F1,6BP) and plays a central role in the glycolytic pathway of prokaryotes and
60 eukaryotes. The enzymatic step catalysed by PFK is conserved in most organisms from Eukarya,
61 Bacteria and Archaea. Despite an enzyme mechanism that has been conserved for over 2 billion
62 years, different PFK families have evolved interestingly diverse regulatory mechanisms associated
63 with considerable differences in protein sequence and architecture. There is increasing interest in
64 PFK as a drug target in human diseases, including diabetes (1) and cancer (2,3). Additionally,
65 glycolysis is a valid therapeutic target for killing pathogens that rely exclusively on glucose catabolism
66 for their ATP supply; previous work has shown the effectiveness of this approach against
67 trypanosomatid parasites (4). PFKs from the three trypanosomatid species that cause significant
68 mortality and morbidity: *Trypanosoma brucei* (Human African Trypanosomiasis), *T. cruzi* (Chagas
69 disease), and *Leishmania* spp. (Leishmaniasis) are all potential drug targets.

70
71 Two main evolutionary groups of PFK are distinguished by their phospho-donor substrates. The
72 pyrophosphate-dependent group uses inorganic pyrophosphate (PPi) as the phospho donor and is
73 found in plants and certain protists, including amoeba and bacteria. The second group uses ATP as
74 the phospho donor and is found in many other bacteria and protists, plants, and all vertebrates (note
75 that plants usually contain PFKs from both groups). Phylogenetic and structural analyses
76 demonstrate that the two groups evolved from a common ancestor, though amino acid sequence
77 identities are low (~25%) (5). Despite these differences, there are similarities in catalytic mechanism;
78 in one interesting case the PP_i-PFK of *Entamoeba histolytica*, which has a 10⁶ fold preference for
79 inorganic pyrophosphate over ATP, could be converted to an ATP-dependent enzyme by a single
80 mutation (6). This supports the idea that the ATP-dependent PFKs are the primordial form from which,
81 on multiple occasions, the PPi-dependent enzymes evolved. However, the evolutionary path is
82 complex, with amino acid sequence comparisons suggesting the ATP-dependent PFK found in
83 trypanosomatids developed through an ancestral PPi reliant stage before switching back to ATP as a
84 substrate (7,8).

85
86 A biochemically important distinction between the two families is that all PPi-PFKs readily carry out
87 both the forward and reverse enzyme reactions under physiological conditions. The biological
88 consequence is that organisms that use PPi-dependent PFKs for the most part do not require
89 fructose-1,6-bisphosphatase enzymes to carry out the reverse dephosphorylation step required in the
90 gluconeogenic pathway. Possibly because of its ability to carry out the reaction in both directions, the
91 PPi-PFK family shows little evidence of allosteric regulatory mechanisms controlling enzyme activity,
92 though this is not universal (9). In contrast, ATP-dependent PFKs have evolved a wide range of
93 allosteric mechanisms, with associated differences in protein chain lengths and architecture.

94
95 The active form of bacterial ATP-dependent PFKs is a homo-tetramer with subunits of approximately
96 35 kDa. In yeasts, a gene duplication/fusion event yielded double-size chains and these subsequently

97 underwent additional duplications to give an octamer comprised of homologous catalytic and
98 regulatory subunits each with a molecular mass of 110-120 kDa (10). Mammals have tetrameric
99 PFKs, with subunits of 85 kDa. The N-terminal half of the double enzyme was constrained to retain
100 the catalytic function, while the substrate binding sites of the C-terminal half evolved into effector
101 binding sites (11). Higher levels of regulation in mammals are also achieved by three distinct isoforms
102 with varying properties (denoted as PFK-M, PFK-L and PFK-P) which are expressed in a tissue-
103 specific pattern (12). Trypanosomatid PFKs are intermediate in size (~55kDa); these are strictly ATP
104 dependent but have amino acid sequences closer to the PPI family and can therefore be regarded as
105 chimeras. X-ray structures of trypanosomatid PFKs show major differences compared with other ATP-
106 dependent PFKs; in particular, the C-terminal extensions can form long helices, acting as reaching
107 arms to hold the tetramer together (8).

108

109 Structural differences between ATP-dependent PFKs derive from varying requirements for allosteric
110 regulation. The smaller bacterial ATP-dependent PFKs are activated by ADP and GDP alone (13)
111 with *Escherichia coli* PFK used in a definitive study by Monod and co-workers to support the now
112 classic allosteric model of enzyme kinetics (14). In trypanosomatid PFKs AMP is the only known
113 activator while in human PFKs the non-catalytic C-domain of each isoform binds the allosteric
114 activators AMP, ADP and fructose 2,6-bisphosphate (F26BP) (15).

115

116 The evolution of these tightly regulated allosteric effector systems in the ATP-dependent PFK family
117 contrasts with the less regulated bi-directional activity of the PPI-dependent family. For the ATP-
118 dependent PFKs the forward enzymatic reaction is favoured under physiological conditions, often
119 being regarded as an essentially irreversible reaction under normal conditions. Indeed, the reverse
120 reaction ($F16BP + ADP \rightleftharpoons F6P + ATP$) has never been demonstrated for any eukaryotic ATP-
121 dependent PFK, including any of the human isoforms, *in vitro* or *in vivo*. In this paper we demonstrate
122 that the reverse reaction is possible under experimental conditions for all three human PFK isoforms
123 and the three trypanosomatid PFK orthologues, and present the kinetic properties for these reactions.
124 The results suggest that the reverse reaction could occur under certain physiological conditions.

125 **METHODS**

126 The identity of all recombinant PFKs was confirmed by SDS-PAGE showing highly pure PFKs of
127 expected molecular weights (Figure 1). Additionally, western blots and MALDI-TOF mass
128 spectrometry using a Bruker Ultraflex instrument confirmed protein identities (data not shown).

129

130 Production of trypanosomatid phosphofructokinases

131 N-terminally His₆-tagged trypanosomatid PFK DNA sequences, codon optimised for *E. coli*
132 expression, were inserted into pET28a or pDEST17 expression plasmids. The recombinant plasmids
133 were used to transform chemically competent *E. coli* cells which were grown on LB agar plates with
134 corresponding antibiotic (Table 1). Single colonies were inoculated into 500ml media in 2L conical
135 flasks and grown in a shaking incubator at 250 rpm and 37°C to an OD_{600nm} 0.8-0.9, then cold
136 shocked at 4°C for 30 min. PFK expression was induced with 1mM isopropyl β-D-1-
137 thiogalactopyranoside (IPTG) for 16h at 100 rpm and 18°C before harvesting the cells via
138 centrifugation and removal of supernatant.

139

140 Cell pellets from 1L cultures were suspended in 50ml lysis buffer (50 mM TEA, 5 mM MgCl₂, 50 mM
141 KCl, 10% glycerol, pH 7.4), supplemented with Roche cOMplete™ EDTA-free Protease Inhibitor
142 Cocktail and ~5mg bovine pancreas deoxyribonuclease [Sigma-Aldrich D5025]) and lysed with
143 Constant Cell Disruption Systems at 25kPsi and centrifuged. Filtered supernatant was loaded onto a
144 cobalt-charged HiTrap 1ml FF immobilized metal affinity chromatography (IMAC) column (GE
145 Healthcare) equilibrated in wash buffer (50 mM triethanolamine (TEA), 300 mM NaCl, 20 mM
146 imidazole, 10% glycerol, pH 8.0) in a GE Healthcare ÄKTA purifier system at 6°C. Impurities were
147 removed by further wash buffer steps with gradually increasing imidazole concentrations before PFK
148 eluted with elution buffer (50 mM TEA, 300 mM NaCl, 500 mM imidazole, 10% glycerol, pH 8.0). *T.*
149 *brucei* and *T. cruzi* PFK (TbPFK and TcPFK) eluates were loaded onto a HiPrep Sephacryl™ S-200
150 16/60 column (GE Healthcare), pre-equilibrated with gel filtration buffer (20 mM TEA, 5 mM MgCl₂, 50
151 mM KCl, 10% glycerol, pH 7.4) and tetrameric fractions eluted with 1.5 column volumes (CV) of gel
152 filtration buffer. *Leishmania infantum* PFK (LmPFK) IMAC eluates were loaded onto a HiPrep 26/10
153 Desalting column (GE Healthcare) pre-equilibrated with gel filtration buffer and eluted using 1.5 CV
154 gel filtration buffer. Samples were concentrated to 1mg/ml with Vivaspin® 20ml 30,000kDa Molecular
155 Weight Cut-Off (MWCO) spin concentrators. Aliquots were flash-frozen and stored at -80°C until
156 required. Tag removal was attempted but only partially successful (Figure 1A); tagged protein was
157 therefore used.

158

159 Production of human phosphofructokinases

160 Plasmid pJH71 (16) containing yeast codon optimised cDNA for His₆-tagged PFK-M1, PFK-L1, or
161 PFK-P1 was used to transform PFK-deficient *S. cerevisiae* (16) via electroporation which were
162 subsequently grown on YPDA (yeast extract, peptone, dextrose, adenine broth) agar plates. Colonies
163 were transferred to 2L conical flasks containing 500ml YPDA medium with 50μ/ml carbenicillin and

164 cultures grown using an Infors HT Multitron standard shaking incubator at 30°C and 250rpm before
165 harvesting the yeast via centrifugation and removal of supernatant.

166

167 Cell pellets from 2L cultures were suspended in lysis buffer (50mM TEA, 300mM KCl, 10mM
168 imidazole, 1mM TCEP, 1mM ATP/F6P) supplemented with Roche cOmplete™ EDTA-free Protease
169 Inhibitor Cocktail and ~5mg bovine pancreas deoxyribonuclease) at 8% w/v and lysed with Constant
170 Cell Disruption Systems at 40kPsi and centrifuged. Filtered supernatant was loaded onto a nickel-
171 charged HiTrap 1ml FF IMAC column equilibrated in wash buffer (50mM TEA, 300mM KCl, 10mM
172 imidazole, 1mM TCEP (tris(2-carboxyethyl)phosphine), 1mM ATP/F6P, 10% glycerol) in an ÄKTA
173 purifier system at 6°C. Impurities were removed by further wash buffer steps with gradually increasing
174 imidazole concentrations before PFK eluted with elution buffer (50mM TEA, 300mM KCl, 500mM
175 imidazole, 1mM TCEP, 1mM ATP/F6P). PFK-M was further purified using a GE Healthcare HiPrep
176 Sephacryl S300 16/600 size-exclusion chromatography column pre-equilibrated with gel filtration
177 buffer (50mM TEA, 500mM KCl, 5mM MgCl₂, 1mM TCEP, 1mM ATP/F6P, 10% glycerol). For PFK-L
178 and PFK-P a GE Healthcare Superose 6 10/300 size-exclusion column was used. Samples
179 corresponding to tetrameric protein (340kDa) were pooled and concentrated using a pre-equilibrated
180 20ml 30,000kDa MWCO spin concentrator to above 0.3mg/ml. Aliquots were flash-frozen and stored
181 at -80°C until required. All buffers were at pH 8, except for PFK-M purifications (pH 7.4).

182

183 Demonstration of reverse reaction using an endpoint assay

184 The Promega Kinase-Glo ATP assay system (V6713) was used to measure ATP production in the
185 reverse PFK reaction. Energy of the ATP produced was converted to light via the luciferase/luciferin
186 reaction in an endpoint reaction. 10µl of PFK at 2µg/ml was added to 100µl assay buffer (50mM TEA,
187 10mM MgCl₂, 0.1% w/v BSA, 0.005% TWEEN20, 1% DMSO, pH 7.4) containing 5mM ADP in a white
188 non-binding 96-well plate. Incubation was carried out at 4°C for 20min, followed by 10min at room
189 temperature. 5mM F16BP (final concentration) was added and the plate was then centrifuged at
190 1000rpm for 30 seconds, and further incubated at room temperature for 60 min. 25µl of the “Kinase-
191 Glo reagent” was added to each well for a final incubation period of 30min. Assay output was
192 measured as luminescence using a Molecular Devices Spectramax M5 Multi-Mode Plate Reader and
193 converted to ATP concentrations using control data from a constructed ATP titration curve.

194

195 Determination of kinetic characteristics using an enzyme-linked kinetic assay

196 Conversion of F16BP (Sigma F6803) and ADP (Sigma A4386) to F6P and ATP was measured using
197 an enzyme-linked assay. F6P was converted to glucose 6-phosphate (G6P) by phosphoglucose
198 isomerase (PGI), and subsequently to 6-phosphogluconolactone by glucose-6-phosphate
199 dehydrogenase (G6PD), with concurrent reduction of NAD⁺ to NADH. Formation of NADH was
200 measured via absorbance of UV at 340nm. ATP produced was re-converted into ADP by glycerol
201 kinase (GK) (in the presence of glycerol) to keep the ATP/ADP ratio low.

202

203 15µl of assay buffer (50mM TEA, 100mM KCl, 10mM MgCl₂, 1mM TCEP, 10% glycerol, pH 7.4) was
204 added to 40µl of assay mix (NAD⁺ (Sigma NAD100-RO), G6PD (Sigma G8529), PGI (Sigma P9544),

205 and GK (Sigma G6142), then 20 μ l of ADP titration (or 15mM ADP stock) in a clear 96-well plate. The
206 plate was incubated at 25°C for 2min. 5 μ l of 0.2mg/ml PFK was added and the reaction initiated with
207 20 μ l F16BP titration (or 25mM F16BP stock). UV absorbance at 340nm was measured at 13s
208 intervals for 15min in a Molecular Devices Spectramax M5 Multi-Mode Plate Reader at 25°C.

209
210 Time-dependent absorbance change was converted into rate of NADH oxidation (μ M.s⁻¹) or specific
211 activity (μ mol.min⁻¹.mg⁻¹) using the Beer-Lambert law (molar extinction co-efficient of NADH 6.22mM⁻¹
212 ¹.cm⁻¹). Reaction rates for each well were calculated using an 8-point (104s) rolling average. Kinetic
213 parameters of the steady-state stage of the reaction were determined with GraphPad Prism 7. Non-
214 linear regression analysis was performed on substrate titration data, with curves fitted using allosteric
215 sigmoidal models, enabling determination of kinetic values.

216 RESULTS

217

218 Proof of concept for reversal of direction of PFK reaction

219 Proof of concept for reversal of the direction of the PFK reaction was established with the 'Kinase-
220 Glo'® assay. Figure 2 shows that addition of PFK to F16BP and ADP enabled much greater
221 production of ATP than in control samples alone. Conversion from concentrations in µg/ml to molar
222 concentrations shows that human and trypanosomatid PFKs produce similar amounts of ATP per
223 mole. The yield of ATP from control experiments may derive from spontaneous conversion of ADP
224 into ATP occurring at high ADP concentrations ($2\text{ADP} \rightleftharpoons \text{ATP} + \text{AMP}$). Potential contamination of
225 ADP stocks with ATP was prevented by using Ultrapure ADP (>99% purity; Promega). Minimal
226 concentrations of ATP were present in PFK stocks, as shown by control experiments without F16BP
227 or ADP; amounts were insufficient to confound results (data not shown).

228

229 Kinetic properties for reverse activity by trypanosomatid PFKs

230 An enzyme-linked assay was used to measure F6P production from the reverse reaction catalysed by
231 PFK isoforms. Michaelis-Menten curves using allosteric sigmoidal models were generated for ADP
232 titrations (Figure 3A) and F16BP titrations (Figure 3B). TbPFK is the most active isoform, with the
233 lowest $K_{0.5}^{\text{ADP}}$ and $K_{0.5}^{\text{F16BP}}$ ($K_{0.5}$ defined as concentration of substrate at which half maximal enzyme
234 velocity is reached, analogous to Michaelis-Menten constant [K_M]). TcPFK has similar kinetic
235 parameters to TbPFK. LmPFK has a slightly lower V_{max} and markedly lower affinities for both
236 substrates, in keeping with known lower activities in the forward reaction (17). Full kinetic parameters
237 are listed in Table 2. Control experiments without PFK did not produce significant quantities of ATP
238 (data not shown).

239

240 Both TcPFK and TbPFK reverse reaction kinetics were consistent with allosteric sigmoidal models for
241 F16BP titrations and for ADP titrations, with LmPFK reaction kinetics showing no statistical difference
242 between the Michaelis-Menten and allosteric sigmoidal models; the allosteric sigmoidal model was
243 preferred to retain consistency.

244

245 The reverse PFK reaction can be allosterically modulated in trypanosomatid PFKs

246 AMP is a known activator, and sole physiological allosteric effector, of the forward PFK reaction in
247 trypanosomatids (15). The effect of AMP on the reverse activity of trypanosomatid PFKs was
248 assessed using the enzyme-linked kinetic assay described above. All three trypanosomatid PFKs
249 were activated in the presence of 0.5mM AMP, with the $k_{\text{cat}}/K_{0.5}^{\text{F16BP}}$ value increasing two-fold for
250 TbPFK and TcPFK, and ten-fold for LmPFK (Supplementary Figure 1 and 2). F26BP, a potent
251 activator of the forward reaction in many eukaryotic ATP-dependent PFKs (but not trypanosomatids)
252 and bi-directional PPI-dependent plant PFKs (18) did not have any effect at 1mM concentration.

253

254 A series of allosteric inhibitors deriving from a compound with anti-TbPFK activity (4) were tested for
255 effects on the reverse PFK reaction catalysed by trypanosomatid PFKs. These compounds inhibited

256 the reverse trypanosomatid PFK reaction with similar potencies to the forward reaction (results not
257 shown).

258

259 The reverse PFK reaction in human PFK isoforms

260 Kinetic parameters for human PFK isoforms were determined using the enzyme-linked kinetic assay.
261 Michaelis-Menten curves using allosteric sigmoidal models were generated for ADP titrations (Figure
262 4A) and F16BP titrations (Figure 4B). PFK-M and PFK-L have similar V_{max} values, but PFK-P is much
263 less active. However, PFK-L has much lower affinities for ADP and F16BP than the other isoforms,
264 with the highest $K_{0.5}^{ADP}$ and $K_{0.5}^{F16BP}$ ($K_{0.5}^{ADP}$ for PFK-P not determined). Kinetic parameters are listed
265 in Table 3. Human PFK isoforms were purified in the presence of 1mM ATP, likely degrading to ADP
266 over time; human PFK stocks thus contributed 10-40 μ M extra nucleotide (ATP or ADP) to the assay.
267 Each reaction was therefore normalised against a control reaction that included PFK isoform sample
268 but not exogenous substrate.

269

270 All reverse reaction kinetics are consistent with allosteric sigmoidal models both for F16BP titrations
271 and ADP titrations; PFK-M ADP titrations did not show any statistically significant difference between
272 the two models so the allosteric sigmoidal model was preferred to retain consistency. The reaction
273 obeys allosteric sigmoidal models at ADP concentrations up to 2.5mM.

274

275 PFK-L has low affinity for ADP and F16BP, indicating a reduced propensity for the reverse reaction
276 compared to other isoforms. The sequence identities between the three isoforms range from 68 to
277 71%, with the ATP binding site being 85-90% identical (the F6P binding site has not been fully
278 characterized as yet). It is challenging to interpret these differences in reverse kinetic properties given
279 the lack of precise information about isoform specific tissue locations, with much of the original
280 published data being measured from relatively crude tissue extracts. However, assuming the original
281 conclusions reached in the 1970-80s (19) are broadly accurate in stating that PFK-L is highly
282 expressed in liver tissues (hence the name: PFK-Liver) then the relative inability of PFK-L to catalyse
283 the reverse reaction may relate to the highly gluconeogenic – and FBPase rich - environment in the
284 human liver. The relatively low activity of PFK-P was also observed in the forward reaction (not
285 shown) and may be an intrinsic property resulting from its susceptibility to time and concentration
286 dependent inactivation probably caused by dissociation of the active tetrameric form (20),

287

288 Substrate inhibition of the reverse PFK reaction in human PFK isoforms

289 There is an inhibitory effect at higher concentrations of ADP (above 2mM) for PFK-M, but the effect is
290 not as clearly demonstrated for the other isoforms (Figure 4A). This effect can be seen more clearly
291 when higher concentrations of ADP are investigated (Figure 5). A similar effect is observed at higher
292 concentrations of F16BP (above 5mM) for PFK-M (Figure 4B). Standard Michaelis-Menten or
293 allosteric sigmoidal kinetic models should be used with caution when substrate inhibition is present;
294 however, more complex models did not increase accuracy of data fitting. It is likely that substrate
295 inhibition of the reverse PFK reaction is also present in PFK-L and PFK-P at higher substrate

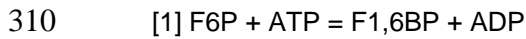
296 concentrations than were used experimentally but to varying degrees, in a similar way that ATP-
297 dependent inhibition differentially affects the forward reaction in each isoform (21). The rationale for
298 substrate inhibition of the reverse reaction remains uncertain. It may be analogous to substrate
299 inhibition by ATP in the forward reaction, which enables finer control of the glycolytic flux (22), though
300 it would be surprising if such an effect had been evolutionary advantageous given the presumed small
301 effect on fitness of precise control of the reverse reaction. High ADP/ATP ratios may enable sufficient
302 ATP production to allow the forward reaction to occur simultaneously; this possibility was reduced –
303 but necessarily eliminated - by adding an excess of glycerol kinase in the presence of glycerol.

304 **DISCUSSION**

305

306 The experiments presented in this paper provide the first kinetic data on the reverse PFK reaction by
307 eukaryotic ATP-dependent phosphofructokinases. The basis for the doctrine that PFK acts only in a
308 forward direction derives from ΔG° being highly favourable for the forward reaction.

309



311

312 $\Delta G^\circ = -3.4 \text{ kcal.mol}^{-1}$ as calculated from the free energies of formation for the products under
313 standard conditions and 1M concentrations (23). The free energy of the reaction under different
314 cellular conditions can be estimated from [2], where the reaction quotient Q is the ratio of
315 concentrations of available products and reactants [3].

316

317 [2] $\Delta G = \Delta G^\circ + RT \ln Q$

318 [3] $Q = \frac{[ADP].[F16BP]}{[ATP].[F6P]}$

319

320 Estimated cellular concentrations of reactants and products for human and trypanosomes are given in
321 Table 4 and can be used to calculate the reaction quotients (Q), the free energy (ΔG), and the
322 equilibrium constant (K), for the PFK reaction in each of the tissue types. For the reverse PFK
323 reaction [1] to take place, ΔG needs to be greater than 0: ($\Delta G^\circ + RT \ln Q > 0$). Substituting
324 appropriate values ($\Delta G^\circ = -3.4 \text{ kcal.mol}^{-1}$ and $RT = 0.543 \text{ kcal.mol}^{-1}$) we can solve for reaction
325 quotient Q ($\frac{[ADP].[F16BP]}{[ATP].[F6P]}$) to show that Q must be greater than 500. In other words, a
326 net reverse reaction will only be energetically favourable when the relative concentration of products
327 (F16BP & ADP) is at least 500-fold greater than that of the substrates (F6P & ATP).

328

329 As shown in Table 4, the concentrations of substrates and products measured in different cell types
330 give estimated reaction quotients of 0.07-0.85 in human tissues and 0.4 in trypanosomatid
331 glycosomes. Additional experimental measurements of muscle from various species, including
332 insects, fish and mammals give ATP/ADP ratios ranging from 11:1 to 1:1 and an average reaction
333 quotient (Q) of 0.42 for their PFKs (24). These Q low values show that in most organisms PFK is
334 working far from the reaction's equilibrium. Further experimental studies using mass spectrometry to
335 estimate forward and reverse flux of each step in glycolysis in yeast, *E. coli* and a mammalian kidney
336 cell line (25) identified PFK as an almost exclusively forward driven glycolytic step in all cells. The
337 measured $\Delta G = -3.2 \text{ kcal.mol}^{-1}$ for PFK in the kidney cell estimated the reverse flux of PFK to be less
338 than 0.7% of the forward flux, with the authors concluding that (under steady state conditions with
339 cells grown in high glucose media) "phosphofructokinase functions as a classic irreversible step". Our
340 data show that for human cells, the measured $K_{0.5}^{ADP}$ values for the reverse reaction (Table 3)
341 exceeds the cytosolic concentrations of ADP (Table 4), but as steady-state concentrations of F16BP
342 are lower than the $K_{0.5}^{F16BP}$ values, it seems likely that under steady state conditions the reverse
343 reaction would indeed be inefficient. However cells can be subjected to extreme conditions of stress

344 and nutrient deprivation and the PFK reverse flux may be very different in non-steady state, glucose-
345 poor conditions and Q values of 500 or above could easily be achieved if ATP or G6P were
346 (transiently) depleted.

347

348 Despite the apparently high energetic barrier, the reverse reaction for ATP-dependent PFK is possible
349 in cells under certain conditions. Experimentally, the reverse reaction was first shown *in vitro* in *E.*
350 *coli* PFK at high ADP and F16BP concentrations (26). Kinetic parameters were determined as K_M^{F16BP}
351 of 398 μ M at 2mM ADP and K_M^{ADP} 50 μ M at saturating concentrations of F16BP. The kinetic
352 parameters suggest generally tighter F16BP and ADP binding compared with the PFK isoforms
353 presented here (Tables 2 and 3) but are not far removed from the kinetic values for PFK-M and this
354 leaves open the question whether there are ever cellular conditions when the reverse reaction could
355 occur.

356

357 Metabolite concentrations vary widely between individuals (27) and these differences will be
358 exaggerated further under conditions of metabolic stress. Low concentrations of aldehyde severely
359 deplete ATP levels (28); cells infected with viruses (29) and necrotic cancer cells (30) have also
360 shown large variations in ADP:ATP ratios. Cells also undergo programmed responses when adapting
361 to new states invoked by events including cell division, apoptosis or nutritional stress which involve
362 concerted changes in activities for families of enzymes (so called 'allostatic changes') (31). The
363 transition between these states frequently necessitates large swings in metabolite concentrations.
364 One such example is the transition from glycolysis to gluconeogenesis triggered by large changes in
365 the ATP:ADP ratio. There will be a lag period whilst waiting for upregulation of FBPase (the
366 gluconeogenic protein that carries out the reverse PFK reaction but not coupled to ATP formation) by
367 increasing transcription/translation or by post-translational modification. During this lag period we
368 postulate that substrate concentrations may be sufficiently perturbed to permit PFK reversal, before
369 FBPase activity becomes available. The potential role of the PFK filament assemblies (35) and the
370 existence of the as yet poorly characterised glycosome complex (36) or G-bodies (32) that tunnel
371 substrates with potentially very high effective concentrations also provides a mechanism for achieving
372 non-equilibrium concentrations of substrates sufficient to push PFK into reverse.

373

374 Trypanosomatids have a uniquely interesting way of organising the glycolytic enzymes with the first
375 seven enzymes in the pathway (including PFK) sequestered in glycosomes (33). In the bloodstream
376 form of *T. brucei*, there can be over 60 of these organelles per cell, comprising about 5% of the cell
377 volume (34). Metabolism in the *T. brucei* parasite has been extensively studied and kinetic
378 parameters for the glycolytic enzymes have been incorporated into a sophisticated *in silico*,
379 experimentally validated metabolic model (35,36). Despite the good predictive properties of such
380 models, it remains difficult to determine the concentrations of individual metabolites. A potential
381 complication in parameterising *in silico* models is caused by compartmentalisation in eukaryotic cells,
382 as metabolite concentrations may vary significantly between different types of vesicles.

383

384 An experimental indication that the reverse PFK reaction may be physiologically relevant and play a
385 role in gluconeogenesis in trypanosomes comes from ¹³C labelled glucose LC-MS work in
386 bloodstream forms of *T. brucei* (37). This showed that hexose phosphates can indeed be derived
387 (albeit at a low rate of 2%) from F16BP despite no active form of FBPase being detectable in
388 glycosomes thus possibly indicating reversal of the normal PFK reaction direction. Further
389 biochemical studies suggest that gluconeogenesis occurs after complete knock-out of FBPase
390 (F.Bringaud, personal communication) and leaves open the possibility that the reverse PFK reaction
391 may contribute to this pathway. Gluconeogenesis is also carried out in *Leishmania*, but recent studies
392 (38) showed that *Leishmania* amastigotes in activated macrophages cannot use amino acids, instead
393 relying on glycolysis. It is unlikely that FBPase is active in amastigotes *in vivo*, because as this
394 would lead to ATP loss by futile cycling. A likely scenario is that these leishmanial forms have an
395 inactivated form of FBPase (e.g. by posttranslational modification), and like the bloodstream-form *T.*
396 *brucei* in the presence of abundant glucose, PFK may function in reverse. As for mammalian PFK,
397 the estimated physiological reaction quotient of 0.4 (Table 4) is far below the required reaction
398 quotient (500) for the reverse direction. Nevertheless, measuring accurate intra-glycosomal substrate
399 concentrations is technically difficult, meaning that the *in vivo* reaction quotient inside glycosomes
400 may be significantly different from whole cell data. An analogous situation occurs with the *T. brucei*
401 glycosomal glycerol kinase reaction, for which it is known that reversal occurs *in vivo* with a low
402 ATP/ADP ratio in the organelles (as created under anaerobic conditions) in the presence of glycerol
403 3-phosphate despite the ΔG° being even less favourable than for PFK reversal (39). Furthermore,
404 mutagenesis experiments revealed structural optimisation of this enzyme for catalysis of the reverse
405 reaction (40).

406
407 Our work shows that LmPFK has significantly lower affinities for ADP and F16BP in the reverse
408 reaction compared to the other trypanosomatid PFKs, though it is activated much more by AMP. The
409 rationale for the differences in trypanosomatid PFK kinetic properties may derive from the differing
410 nutritional environments to which each parasite has become adapted. *T. brucei* is exclusively extra-
411 cellular, usually confined to the haemolymphatic circulation and cerebrospinal fluid, whereas *T. cruzi*
412 is both (transiently) bloodstream and intracellular (cytosolic), infecting a wide variety of cells.
413 *Leishmania* parasites are predominantly restricted to macrophage phagolysosomes, where they may
414 become metabolically quiescent resulting in low growth rates (41). In this energy restricted
415 environment, the low-energy signal of rising AMP levels may be more important in stimulating
416 glycolytic or gluconeogenic activity, accounting for the greater sensitivity of LmPFK to AMP.

417
418 The kinetic data for the eukaryotic ATP-dependent PFKs presented in this paper help provide a more
419 detailed understanding of the controls governing the glycolytic and gluconeogenic pathways. They will
420 also provide useful experimental data to feed into the increasingly detailed computational models
421 describing these pathways in mammals (42) and trypanosomes (43). The high reaction quotient (Q)
422 required for the reverse reaction can in principle be attained when ATP has been depleted (< 100 μ M)
423 in the presence of physiologically relevant cellular concentrations of ADP, F6P and F16BP. However,

424 for the human isoforms, the measured $K_{0.5}$ values for F16BP are higher than the measured cellular
425 concentrations. To suggest any physiological relevance for the human isoforms would require the
426 existence of an 'apparent concentration' of F16BP up to ten-fold higher than has been measured; this
427 is potentially achievable by invoking substrate tunnelling or metabolon structures. The kinetic data
428 measured for the trypanosomatid PFKs would (as for the mammalian PFKs) require a significant
429 increase in ADP/ATP ratio for the reverse reaction, though the cellular concentration of F16BP would
430 (unlike the mammalian case) be above the $K_{0.5}$ and sufficient to drive the reaction in the opposite
431 direction. Future more detailed metabolomics studies will continue to deliver more precise data on
432 time-dependent and organelle-dependent metabolite concentrations which will shed more light on the
433 potential physiological relevance of the reverse PFK reaction.

434

435 ACKNOWLEDGEMENTS

436 We thank Professor J Heinisch (Universität Osnabrück) for donation of the vector pJH71 and the
437 double PFK knockout strain of *S. cerevisiae*, and Dr Meng Yuan for his help with the enzyme-linked
438 assay. We also thank the Edinburgh Protein Production Facility for assistance with recombinant
439 protein production.

440

441

442 REFERENCES

- 443 1. Da Silva D, Ausina P, Alencar EM, Coelho WS, Zancan P, Sola-Penna M. Metformin reverses
444 hexokinase and phosphofructokinase downregulation and intracellular distribution in the heart
445 of diabetic mice. *IUBMB Life*. 2012;64(9):766–74.
- 446 2. Granchi C, Minutolo F. Anticancer Agents That Counteract Tumor Glycolysis. *ChemMedChem*.
447 2012;7(8):1318–50.
- 448 3. Rajeshkumar N V, Yabuuchi S, Pai SG, Oliveira E De, Jurre J. Treatment of pancreatic cancer
449 patient-derived xenograft panel with metabolic inhibitors reveals efficacy of phenformin. *Clin*
450 *Cancer Res*. 2017;23(18):5639–47.
- 451 4. Brimacombe KR, Walsh MJ, Liu L, Vásquez-Valdivieso MG, Morgan HP, McNae I, et al.
452 Identification of ML251, a potent inhibitor of *T. brucei* and *T. cruzi* phosphofructokinase. *ACS*
453 *Med Chem Lett*. 2014;5(1):12–7.
- 454 5. Moore SA, Ronimus RS, Roberson RS, Morgan HW. The structure of a pyrophosphate-
455 dependent phosphofructokinase from the Lyme disease spirochete *Borrelia burgdorferi*.
456 *Structure*. 2002;10(5):659–71.
- 457 6. Chi A, Kemp RG. The primordial high energy compound: ATP or inorganic pyrophosphate? *J*
458 *Biol Chem*. 2000;275(46):35677–9.
- 459 7. Michels PA, Chevalier N, Opperdoes FR, Rider MH, Rigden DJ. The glycosomal ATP-
460 dependent phosphofructokinase of *Trypanosoma brucei* must have evolved from an ancestral
461 pyrophosphate-dependent enzyme. *Eur J Biochem*. 1997;250(3):698–704.
- 462 8. Mcnae IW, Martinez-oyanedel J, Keillor JW, Michels PAM, Fothergill-gilmore LA, Walkinshaw
463 MD. The Crystal Structure of ATP-bound Phosphofructokinase from *Trypanosoma brucei*
464 Reveals Conformational Transitions Different from those of Other Phosphofructokinases. *J Mol*
465 *Biol* [Internet]. 2009;385(5):1519–33. Available from:
466 <http://dx.doi.org/10.1016/j.jmb.2008.11.047>
- 467 9. Mertens E, De Jonckheere J, Van Schaftingen E. Pyrophosphate-dependent
468 phosphofructokinase from the amoeba *Naegleria fowleri*, an AMP-sensitive enzyme. *Biochem*
469 *J*. 1993;292 (Pt 3):797–803.

- 470 10. Poorman RA, Randolph A, Kemp RG, Heinrichson RL. Evolution of phosphofructokinase - Gene
471 duplication and creation of new effector sites. *Nature*. 1984;309(5967):467–9.
- 472 11. Baptiste E, Moreira D, Philippe H. Rampant horizontal gene transfer and phospho-donor
473 change in the evolution of the phosphofructokinase. *Gene*. 2003;318(1–2):185–91.
- 474 12. Dunaway G a, Kasten TP, Sebo T, Trapp R. Analysis of the phosphofructokinase subunits and
475 isoenzymes in human tissues. *Biochem J*. 1988 May;251(3):677–83.
- 476 13. Schirmer T, Evans PRP. Structural basis of the allosteric behaviour of phosphofructokinase.
477 *Nature* [Internet]. 1990;343(6254):140–5. Available from:
478 <http://www.nature.com/doi/10.1038/343140a0>
- 479 14. Blangy D, Buc H, Monod J. Kinetics of the allosteric interactions of phosphofructokinase from
480 *Escherichia coli*. *J Mol Biol*. 1968;31(1):13–35.
- 481 15. Schöneberg T, Kloos M, Brüser A, Kirchberger J, Sträter N. Structure and allosteric regulation
482 of eukaryotic 6-phosphofructokinases. *Biol Chem*. 2013;394(8):977–93.
- 483 16. Heinisch J. Construction and physiological characterization of mutants disrupted in the
484 phosphofructokinase genes of *Saccharomyces cerevisiae*. *Curr Genet*. 1986;11(3):227–34.
- 485 17. Berens R, Marr J. Phosphofructokinase of *Leishmania donovani* and *Leishmania braziliensis*
486 and its Role in Glycolysis. *J Protozool*. 1977;
- 487 18. Mertens E. Pyrophosphate-dependent phosphofructokinase, an anaerobic glycolytic enzyme?
488 *FEBS Lett*. 1991;285(1):1–5.
- 489 19. Kahn A, Meienhofer MC, Cottreau D, Lagrange JL, Dreyfus JC. Phosphofructokinase (PFK)
490 isozymes in man. I. Studies of adult human tissues. *Hum Genet*. 1979 Apr;48(1):93–108.
- 491 20. Fernandes PM, Yen L-H, Kinkead J, McNae I, Michels P, Walkinshaw MD. Effect of ligands
492 and redox state on phosphofructokinase quaternary structure and enzymatic activity. *Lancet*.
493 2017;389:S36.
- 494 21. Nakajima H, Raben N, Hamaguchi T, Yamasaki T. Phosphofructokinase deficiency; past,
495 present and future. *Curr Mol Med* [Internet]. 2002;2(2):197–212. Available from:
496 <http://www.ncbi.nlm.nih.gov/pubmed/11949936>
- 497 22. Meienhofer MC, Cottreau D, Dreyfus JC, Kahn A. KINETIC PROPERTIES OF HUMAN F4
498 PHOSPHOFRUCTOKINASE. *FEBS Lett*. 1980;110(2):219–22.
- 499 23. Berg J, Tymoczko J, Stryer L. *Biochemistry* (5th ed). 5th ed. W.H. Freeman & Co Ltd; 2001.
500 436-7 p.
- 501 24. Beis I, Newsholme EA. The contents of adenine nucleotides, phosphagens and some
502 glycolytic intermediates in resting muscles from vertebrates and invertebrates. *Biochem J*
503 [Internet]. 1975;152(1):23–32. Available from:
504 <http://www.pubmedcentral.nih.gov/articlerender.fcgi?artid=1172435&tool=pmcentrez&rendertype=abstract>
505
- 506 25. Park J, Rubin S, Xu Y, Amador-Noguez D, Fan J, Shlomi T, et al. Metabolite concentrations,
507 fluxes, and free energies imply efficient enzyme usage. *Nat Chem Biol*. 2016;12(7):277–94.
- 508 26. Auzat I, Garel J. pH dependence of the reverse reaction catalyzed by phosphofructokinase I
509 from *Escherichia coli*: Implications for the role of Asp 127. *Protein Sci*. 1992;1:254–8.
- 510 27. Saude EJ, Adamko AED, Rowe AEBH, Marrie T, Sykes AEBD. Variation of metabolites in
511 normal human urine. *Metabolomics*. 2007;3:439–51.
- 512 28. Tiffert T, Garcia-Sancho J, Lew V. Irreversible ATP depletion caused by low concentrations of
513 formaldehyde and of calcium-chelator esters in intact human red cells. *Biochim Biophys Acta*.
514 1984;773:143–56.
- 515 29. Ando T, Imamura H, Suzuki R, Aizaki H, Watanabe T, Wakita T, et al. Visualization and
516 measurement of ATP levels in living cells replicating hepatitis C virus genome RNA. *PLoS*

- 517 Pathog. 2012;8(3).
- 518 30. Bradbury DA, Simmons TD, Slater KJ, Crouch SPM. Measurement of the ADP:ATP ratio in
519 human leukaemic cell lines can be used as an indicator of cell viability, necrosis, and
520 apoptosis. *J Immunol Methods*. 2000;240:79–92.
- 521 31. Bermejo-Nogales A, Nederlof M, Benedito-Palos L, Ballester-Lozano GF, Folkedal O, Olsen
522 RE, et al. Metabolic and transcriptional responses of gilthead sea bream (*Sparus aurata* L.) to
523 environmental stress: New insights in fish mitochondrial phenotyping. *Gen Comp Endocrinol*
524 [Internet]. 2014;205:305–15. Available from: <http://dx.doi.org/10.1016/j.ygcen.2014.04.016>
- 525 32. Jin M, Fuller GG, Han T, Inoki K, Klionsky DJ, Kim JK, et al. Glycolytic Enzymes Coalesce in G
526 Bodies under Hypoxic Stress Article Glycolytic Enzymes Coalesce in G Bodies under Hypoxic
527 Stress. *Cell Rep* [Internet]. 2017;20(4):895–908. Available from:
528 <http://dx.doi.org/10.1016/j.celrep.2017.06.082>
- 529 33. Bakker BM, Mensonides FIC, Teusink B, van Hoek P, Michels PAM, Westerhoff H V.
530 Compartmentation protects trypanosomes from the dangerous design of glycolysis. *Proc Natl*
531 *Acad Sci U S A* [Internet]. 2000;97(5):2087–92. Available from:
532 <http://www.pnas.org/cgi/doi/10.1073/pnas.030539197>
- 533 34. Tetley L, Vickerman K. The glycosomes of trypanosomes: number and distribution as revealed
534 by electron spectroscopic imaging and 3-D reconstruction. *J Microsc* [Internet]. 1991;162(Pt
535 1):83–90. Available from:
536 http://www.ncbi.nlm.nih.gov/entrez/query.fcgi?cmd=Retrieve&db=PubMed&dopt=Citation&list_
537 [uids=1870115](http://www.ncbi.nlm.nih.gov/entrez/query.fcgi?cmd=Retrieve&db=PubMed&dopt=Citation&list_uids=1870115)
- 538 35. Albert M-A, Haanstra JR, Hannaert V, Van Roy J, Opperdoes FR, Bakker BM, et al.
539 Experimental and in Silico Analyses of Glycolytic Flux Control in Bloodstream Form
540 *Trypanosoma brucei*. *J Biol Chem* [Internet]. 2005;280(31):28306–15. Available from:
541 <http://www.jbc.org/cgi/doi/10.1074/jbc.M502403200>
- 542 36. Bakker BM, Michels PAM, Opperdoes FR, Westerhoff H V. Glycolysis in bloodstream form
543 *Trypanosoma brucei* can be understood in terms of the kinetics of the glycolytic enzymes. *J*
544 *Biol Chem*. 1997;272(6):3207–15.
- 545 37. Creek DJ, Mazet M, Achcar F, Anderson J, Kim DH, Kamour R, et al. Probing the Metabolic
546 Network in Bloodstream-Form *Trypanosoma brucei* Using Untargeted Metabolomics with
547 Stable Isotope Labelled Glucose. *PLoS Pathog*. 2015;11(3):1–25.
- 548 38. Saunders EC, Naderer T, Chambers J, Landfear SM, Mcconville MJ. *Leishmania mexicana*
549 can utilize amino acids as major carbon sources in macrophages but not in animal models.
550 *Mol Microbiol*. 2018;00:1–16.
- 551 39. Hammond DJ, Aman RA, Wangs CC. The Role of Compartmentation and Glycerol Kinase in
552 the Synthesis of ATP within the Glycosome of *Trypanosoma brucei* ". 1985;15646–54.
- 553 40. Balogun EO, Inaoka DK, Shiba T, Kido Y, Tsuge C, Nara T, et al. Molecular basis for the
554 reverse reaction of African human trypanosomes glycerol kinase. *Mol Microbiol*.
555 2014;94(November):1315–29.
- 556 41. McConville MJ, Saunders EC, Kloehn J, Dagley MJ. *Leishmania* carbon metabolism in the
557 macrophage phagolysosome- feast or famine. *F1000Research*. 2015;4:1–11.
- 558 42. Marín-Hernández A, López-Ramírez SY, Del Mazo-Monsalvo I, Gallardo-Pérez JC,
559 Rodríguez-Enríquez S, Moreno-Sánchez R, et al. Modeling cancer glycolysis under
560 hypoglycemia, and the role played by the differential expression of glycolytic isoforms. *FEBS J*.
561 2014;281(15):3325–45.
- 562 43. Achcar F, Fadda A, Haanstra JR, Kerkhoven EJ, Kim DH, Leroux AE, et al. The Silicon
563 *Trypanosome*. A Test Case of Iterative Model Extension in Systems Biology. *Adv Microb*
564 *Physiol*. 2014;64:115–43.
- 565

TABLES

Table 1 Expression conditions for trypanosomatid PFKs in *E. coli*

	<u>DNA source</u> <u>strain</u>	<u>Expression</u> <u>plasmid</u>	<u>Expression</u> <u>cell line</u>	<u>Antibiotic</u>	<u>Media</u>
<i>T. b. brucei</i>	Lister 427	pET28a	C41 (DE3)	Kanamycin	2xYT broth
<i>T. cruzi</i>	CL Brener	pET28a	BL21 (DE3)	Kanamycin	Superbroth
<i>L. infantum</i>	JPCM5	pDEST17	C41 (DE3)	Carbenicillin	LB broth

Table 2 Kinetic parameters for trypanosomatid PFKs in the reverse reaction. Values are mean averages (+/- standard error of mean; n = 3). Large standard errors for TcPFK data result from varying degree of fit of non-linear regression sigmoidal models, despite narrow error bars apparent in Figure 4.

	V_{max} ($\mu\text{moles}/\text{min}.\text{mg}$)	$K_{0.5}^{ADP}$ (μM)	$K_{0.5}^{F16BP}$ (μM)	h (ADP)	h (F16BP)
TcPFK	4.77 (1.37)	1768 (2238)	1540 (153)	0.51 (0.14)	1.72 (0.22)
TbPFK	4.22 (0.28)	1382 (275)	1287 (202)	0.83 (0.07)	0.86 (0.06)
LmPFK	3.79 (0.69)	3137 (1084)	2495 (624)	1.42 (0.37)	1.71 (0.65)

Table 3 PFK-L has the lowest affinity for F16BP in the reverse reaction. (Mean average values with SEM values in brackets; n = 3).

	V_{max} ($\mu\text{moles}/\text{min.mg}$)	$K_{0.5}^{ADP}$ (μM)	$K_{0.5}^{F16BP}$ (μM)	h (ADP)	h (F16BP)
PFK-M	0.63 (0.05)	66.8 (13.4)	804 (66.1)	0.71 (0.22)	1.83 (0.23)
PFK-L	0.62 (0.01)	344.9 (36.4)	2100 (78.4)	1.39 (0.17)	2.49 (0.19)
PFK-P	0.22 (0)	ND	717.8 (58.1)	ND	1.35 (0.12)

Table 4: Concentrations of substrates and products of PFK in various mammalian tissues. ΔG calculated from equation (2) using $RT = 0.543 \text{ kcal.mol}^{-1}$ where R is the gas constant ($1.987 \text{ cal.mol}^{-1}\text{K}^{-1}$) and T = temperature (293K). Equilibrium constant K is calculated from $K = \exp(-\Delta G/RT)$. References for concentrations (directly measured in non-italicised text, derived from models based on whole cell lysate data in italicised text): ^a (Minakami and Yoshikawa 1966); ^b (Beis and Newsholme 1975); ^c (Zalitis and Oliver 1967); ^d (Lowry and Passonneau 1964); ^e (Spolter, Adelman, and Weinhouse 1965); ^f (Rao and Oesper 1961); ^g (Hisanaga, Onodera, and Kogure 1986); ^h (Bakker, Westerhoff, and Michels 1995); ⁱ (Graven et al. 2014).

	Erythrocyte	Muscle	Brain	<i>T. brucei</i> glycosome
[ATP] μM	1850 ^a	4990 ^b	3325 ^g	3870 ⁱ
[ADP] μM	180 ^a	600 ^f	309 ^g	1315 ⁱ
[F6P] μM	15.7 ^a	110 ^c	27 ^d	2400 ^h
[F16BP] μM	7 ^a	32 ^e	200 ^d	1900 ^h
Q (derived)	0.04	0.03	0.69	0.27
ΔG (kcal/mol)	-5.09	-5.21	-3.6	-4.7

FIGURES

Figure 1. SDS-PAGE gels (4-20%) showing A) trypanosomatid PFKs were produced at high purity but removal of tags was only partially successful and B) human PFK isoforms were produced at high purity but with anomalous migration of PFK-L. Tagged enzymes were used for all experiments due to incomplete tag cleavage and reduction of enzyme activity after cleavage (data not shown), likely secondary to conditions required to remove tag. Ladder markers are in kDa.

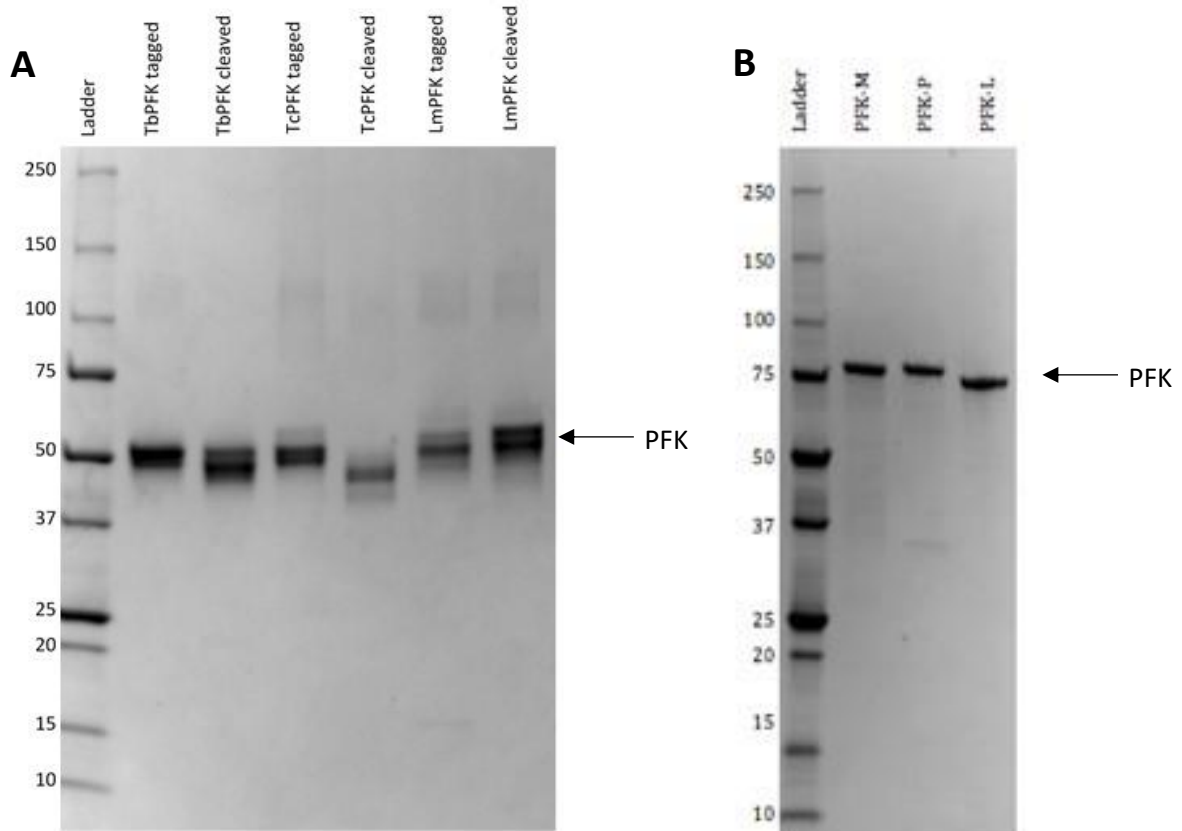


Figure 2. ATP is produced by PFKs from ADP and F16BP using an endpoint assay (ADP 5mM, F16BP 5mM, error bars are standard deviations; n = 2).

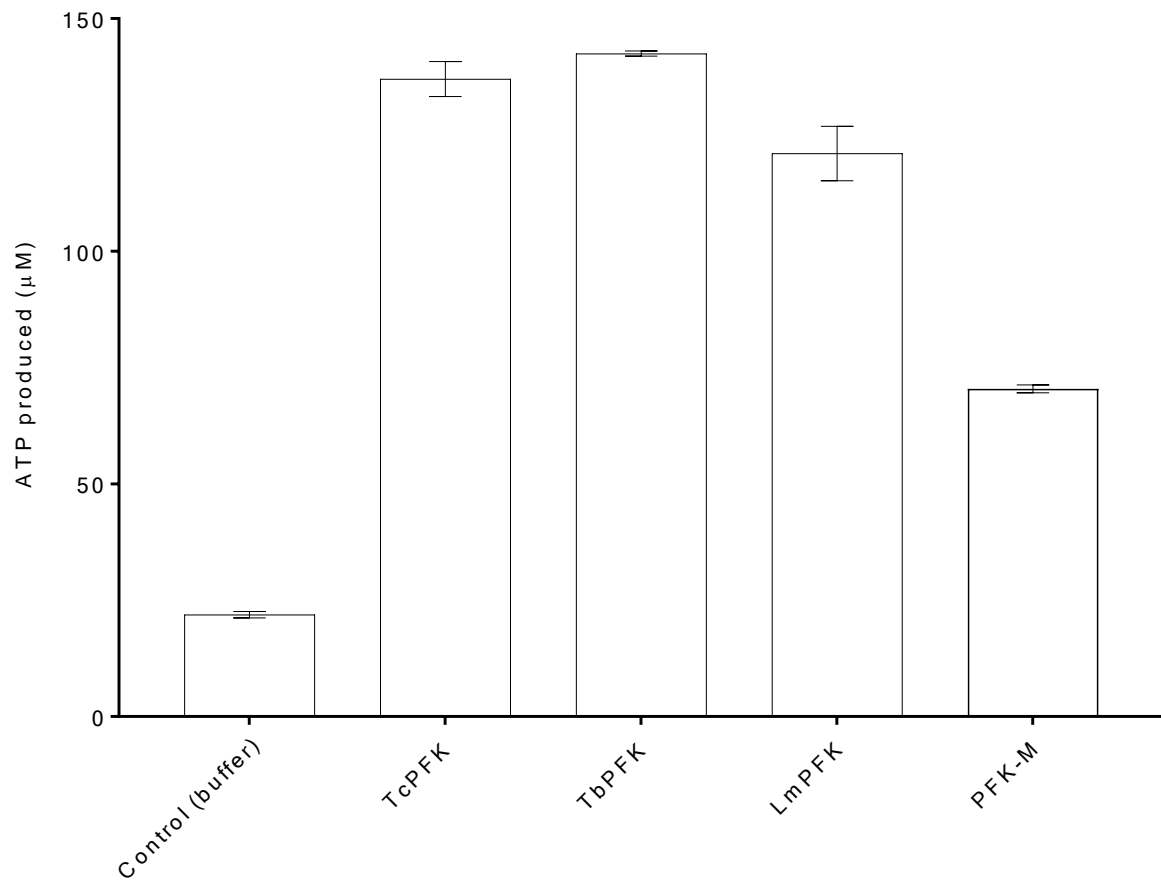


Figure 3.

A) Trypanosomatid PFKs have different kinetic responses for ADP titrations (F16BP 5mM).

B) Trypanosomatid PFKs have different kinetic responses for F16BP titrations (ADP 3mM).

(error bars are standard deviations, n = 3).

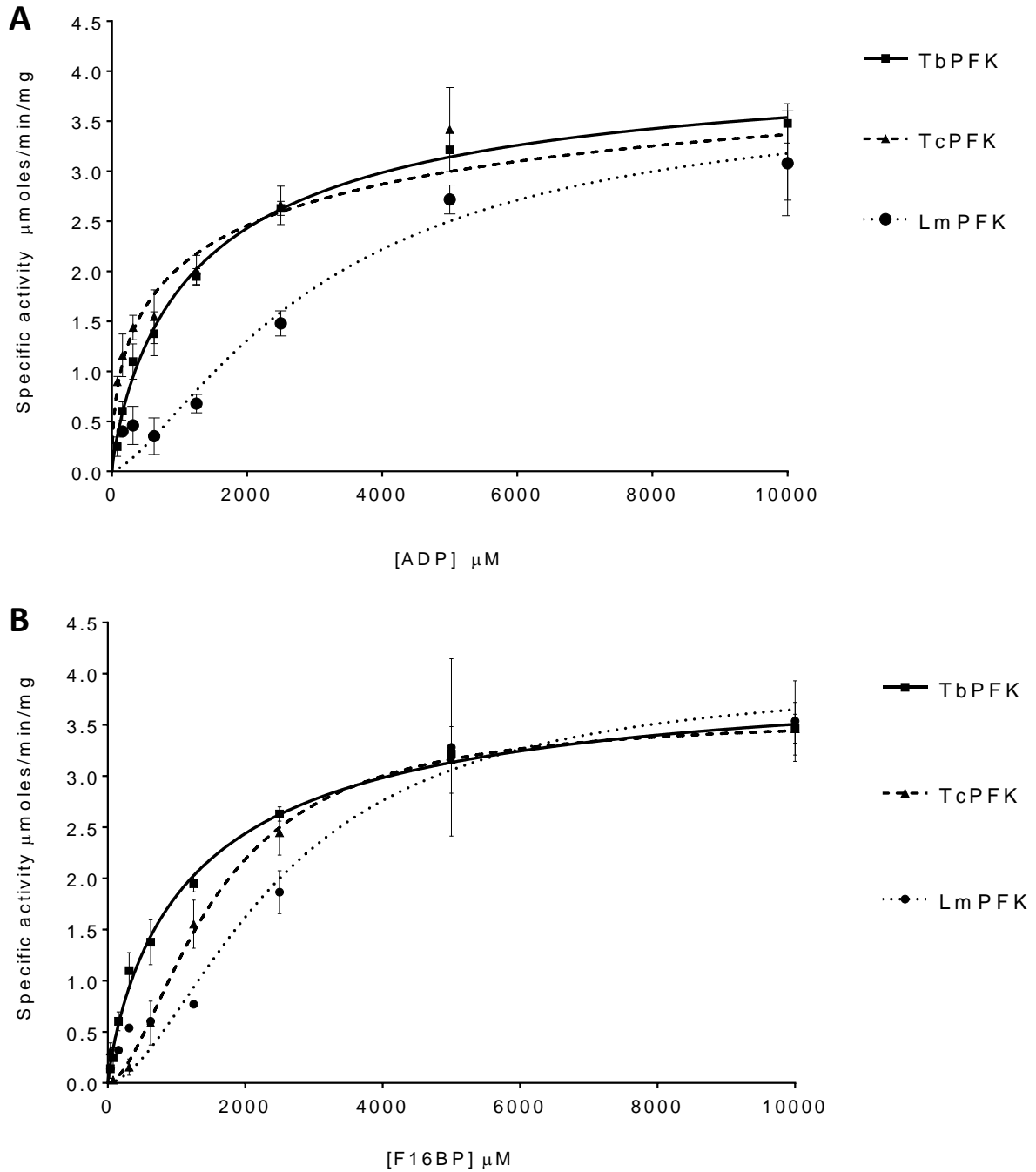


Figure 4.

A) Human PFK isoforms have different kinetic responses for ADP titrations (F16BP 5mM)

B) Human PFK isoforms have different kinetic responses for F16BP titrations (ADP 3mM)

PFK-P data are missing for 4A due to lack of enzyme stability under these assay conditions. (Error bars are standard deviations, n = 3, isoforms were individually normalised to highest specific activity).

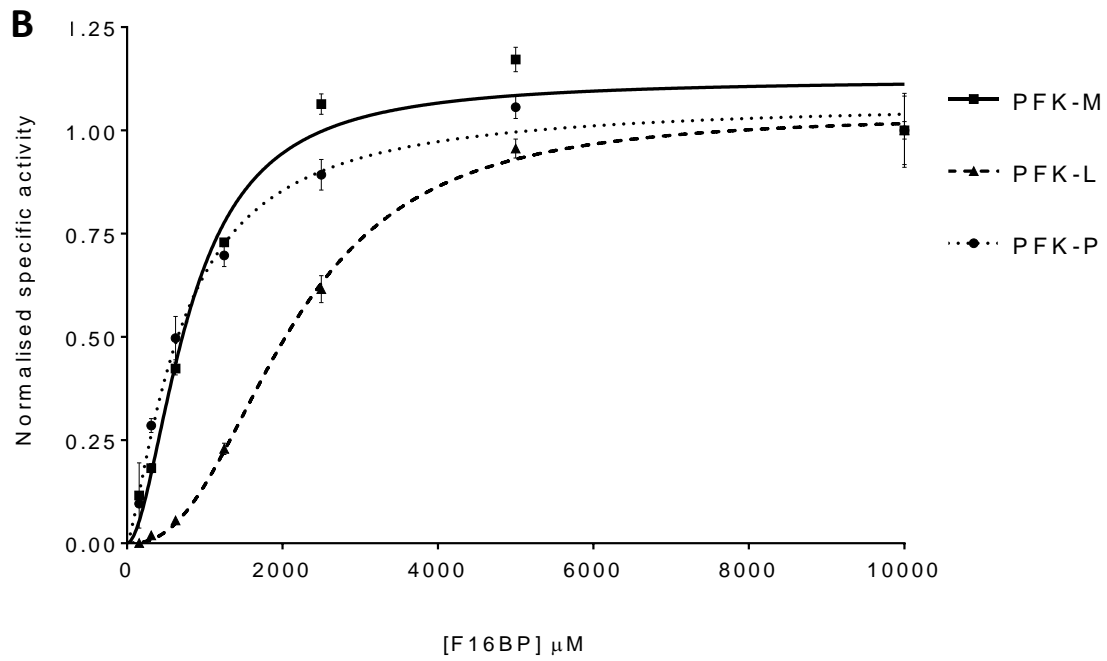
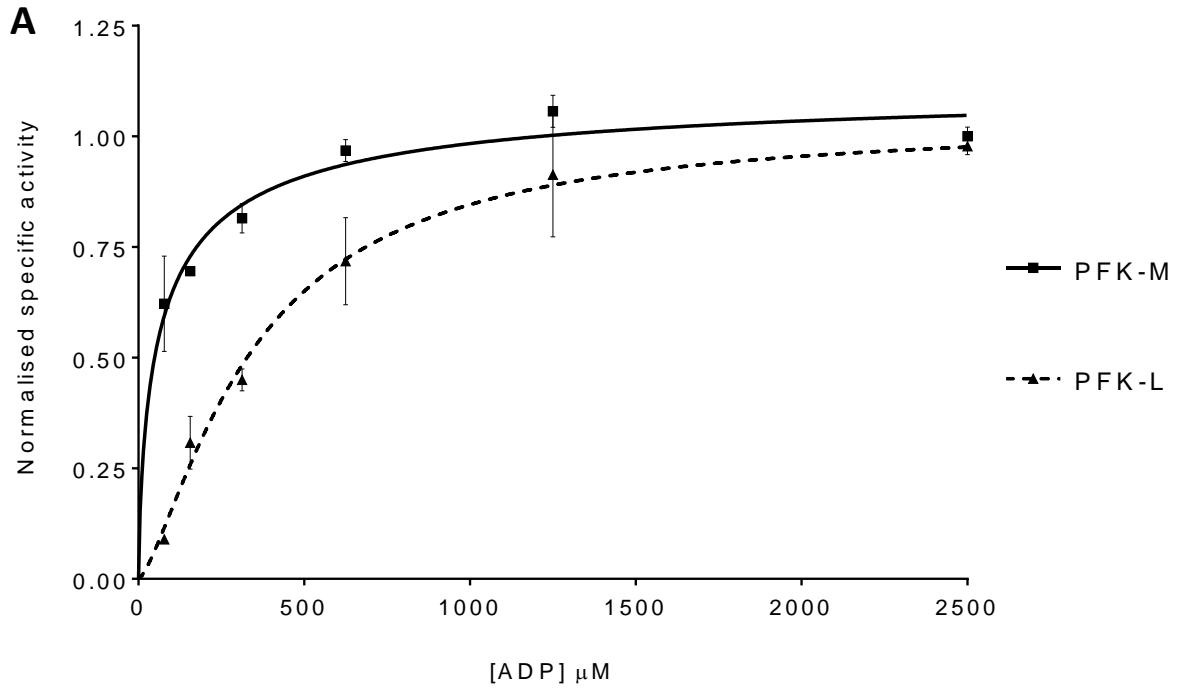
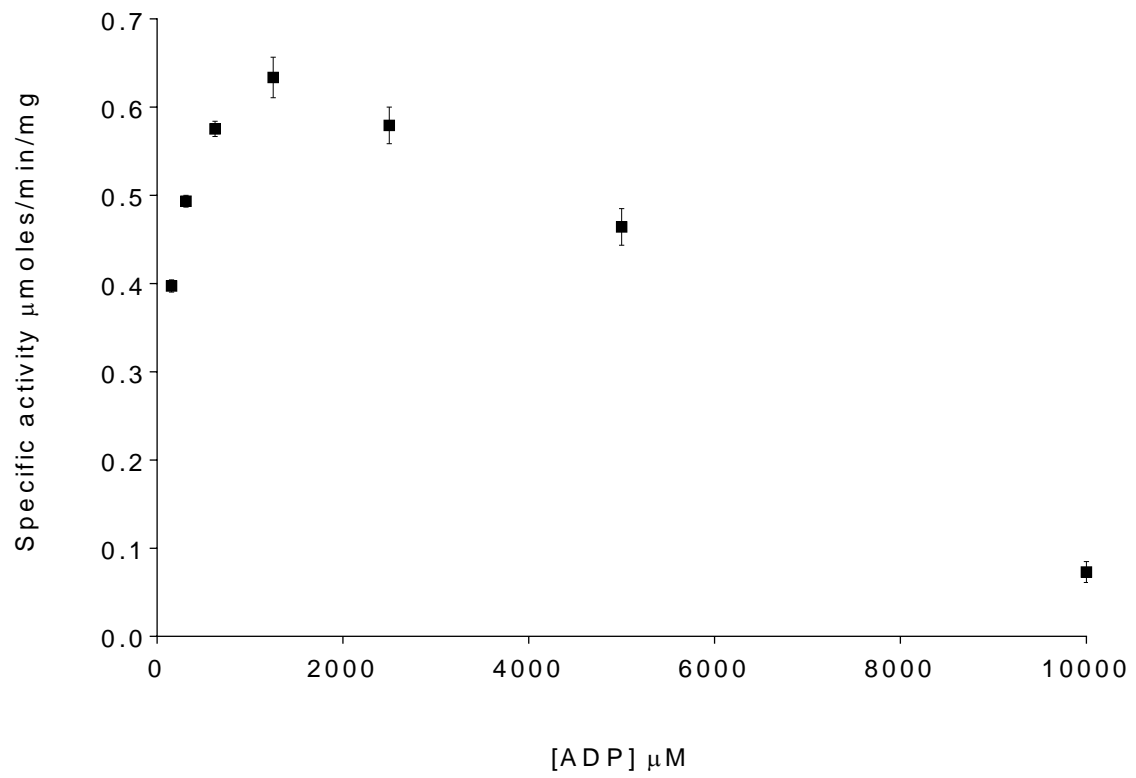


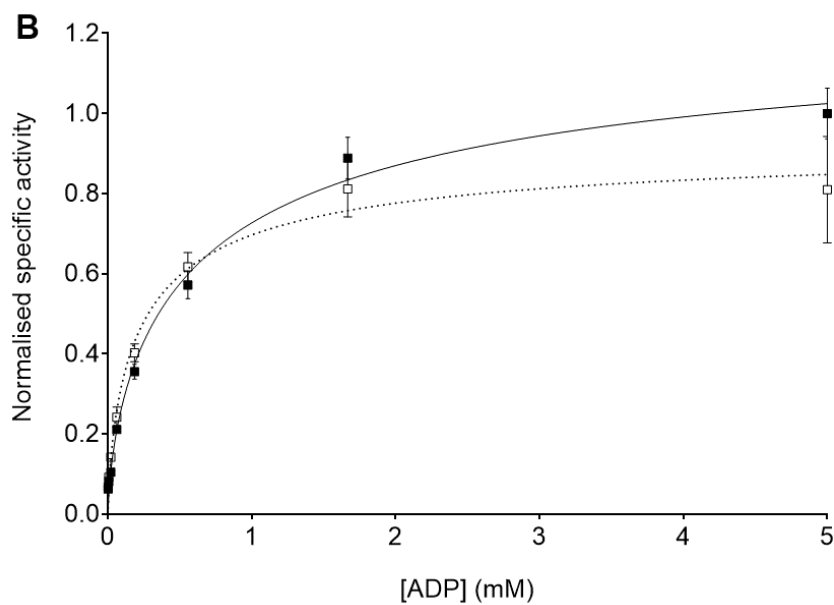
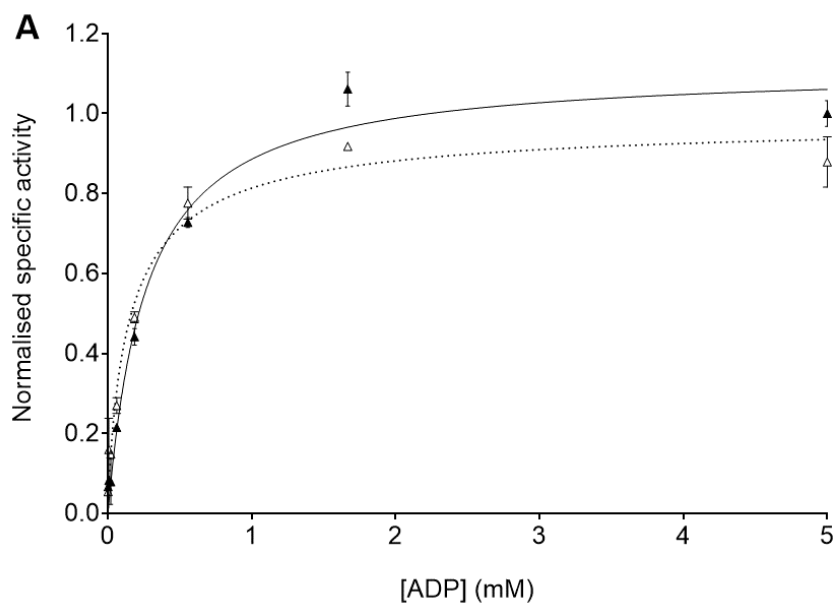
Figure 5. High concentrations of ADP inhibit the reverse reaction for PFK-M. (Error bars are standard deviations; n = 3).

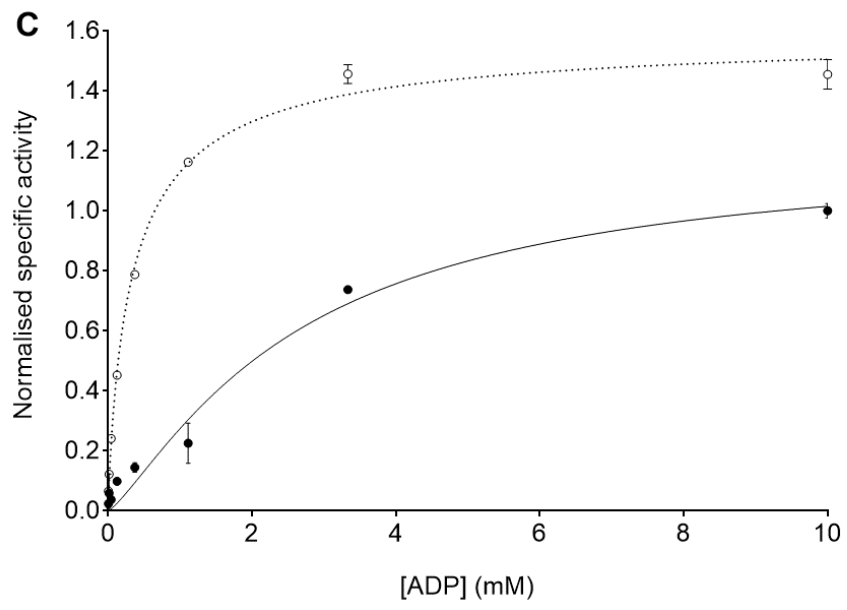


SUPPLEMENTARY FIGURE 1

- A) AMP activates TcPFK with respect to ADP titrations (F16BP 10mM). 0mM AMP (solid triangles ▲ with solid line), 0.5mM AMP (open triangles △ with dotted line)
- B) AMP activates TbPFK with respect to ADP titrations (F16BP 10mM). 0mM AMP (solid squares ■ with solid line), 0.5mM AMP (open squares □ with dotted line)
- C) AMP activates LmPFK with respect to ADP titrations (F16BP 20mM). 0mM AMP (solid circles ● with solid line), 0.5mM AMP (open circles ○ with dotted line)

(n= 2, error bars are standard deviations, results for each enzyme normalised to highest specific activity without AMP present).





SUPPLEMENTARY FIGURE 2

- A) AMP activates TcPFK with respect to F16BP titrations (ADP 5mM). 0mM AMP (solid triangles ▲ with solid line), 0.5mM AMP (open triangles △ with dotted line)
- B) AMP activates TbPFK with respect to F16BP titrations (ADP 5mM). 0mM AMP (solid squares ■ with solid line), 0.5mM AMP (open squares □ with dotted line)
- C) AMP activates LmPFK with respect to F16BP titrations (ADP 10mM). 0mM AMP (solid circles ● with solid line), 0.5mM AMP (open circles ○ with dotted line)

(n= 2, error bars are standard deviations, results for each enzyme normalised to highest specific activity without AMP present).

